Pergamon

Tetrahedron, Vol. 53, No. 29, pp. 10051-10070, 1997

0040-4020/97 $17.00 + 0.00

PII: S0040-4020(97)00347-5

CIDNP Study and Ab-Initio Calculations of Rigid Vinylcyclopropane Systems: Evidence For Delocalized "Ring-Closed" Radical Cations

Heinz D. Roth, Hengxin Weng and Torsten Herbertz*

Rutgers University, Department of Chemistry

New Brunswick, New Jersey, USA

Abstract: The radical cations of three terpenes, sabinene, **1**, and α-, **2**, and β-thujene, **3**, containing vinylcyclopropane functions held rigidly in either an anti- or syn-orientation, have been elucidated by CIDNP studies. The structures assigned to these species are discussed in view of their reactivities and compared with three simplified radical cations, 2-methylenebicyclo[3.1.0]hexane, **4**, bicyclo[3.1.0]hex-2-ene, **5**, and 5-methylbicyclo[3.1.0]hex-2-ene, **6**, calculated by *ab initio* molecular orbital methods.

INTRODUCTION

Conjugative and homoconjugative interactions between strained ring moieties and olefinic fragments in organic radical cations have been the focus of much interest for the past decade.[1,2] In particular EPR and CIDNP spectroscopic studies have been applied to characterize the spin density distributions of radical cations and to deduce changes in the molecular geometry upon oxidation.[1,2] Many reactions of these species result in the release of ring strain,[3] often assisted by a nucleophile.[4] The simplest species containing both an olefinic moiety and a cyclopropane ring, the vinylcyclopropane radical cation, has only recently been characterized in several studies.[5-10] The mass spectrum of this species shows evidence for ring opening to penta-1,3-diene radical cation.[5] Analogous conversions were observed in solution; thus, the radical cation of sabinene, **1**$^{\bullet+}$, undergoes a [1,3] sigmatropic shift (with inversion of stereochemistry at C_1) whereas the radical cation of α-thujene, **2**$^{\bullet+}$, reacts via a [1,3] sigmatropic shift in competition with a homo-[1,5] sigmatropic shift.[6]

Theoretical approaches include an early STO-3G calculation for a vinylcyclopropane radical cation with seriously restricted geometry,[7] more recent INDO calculations[8] and *ab initio* calculations at the MP2/6-31G* and B3LYP/6-31G* level of theory.[9] Also, three radical cations of bicyclo[3.1.0]hex-2-ene and bicyclo[4.1.0]hept-2-ene systems, were characterized by CIDNP experiments.[10] Finally, several 2-*p*-anisyl derivatives undergo electron transfer induced vinylcyclopropane rearrangements.[3h,i]

To gain a deeper understanding of vinylcyclopropane radical cations, we have studied three terpenes, in which the two functionalities are locked in either the *anti*- (viz., 4-methylene-1-isopropylbicyclo[3.1.0]hexane (sabinene, **1**) or the *syn*-orientation (α-thujene, **2**, and β-thujene, **3**). The fixed orientations of the vinyl group relative to the cyclopropane moiety and the different substitution patterns in these substrates allow the detailed evaluation of potential FMO interactions between the cyclopropane and the vinyl groups. The results probe the significance of such factors as orbital overlap and charge stabilization in the radical cations[4e] and the release of ring strain in their formation or in their reactions. In this paper we discuss the structures of the three radical cations, **1**$^{\bullet+}$ – **3**$^{\bullet+}$, on the basis of CIDNP results observed during their electron transfer reactions with photo-excited (triplet) chloranil. The CIDNP spectra reveal the relative magnitudes and relative signs for the hyperfine coupling constants (hfcs) of individual nuclei and the spin density distribution in the radical cations.

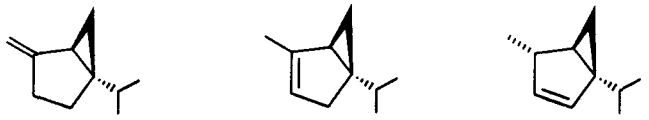

1 **2** **3**

The resulting hyperfine couplings and spin densities are compared with the results of *ab initio* calculations for three radical cations, 2-methylenebicyclo[3.1.0]hexane, **4**, bicyclo[3.1.0]hex-2-ene, **5**, and 5-methylbicyclo[3.1.0]hex-2-ene, **6**.[11] These were calculated with the GAUSSIAN 94 electronic structure programs,[12] using extended basis sets, including p-type polarization functions on carbon (6-31G*), and appropriate levels of electron correlation (MP2). Density functional theory methods (B3LYP)[13] were also applied. The simplified models were chosen to limit the computing resources required; particularly the omission of the isopropyl group reduced the required resources. On the other hand, this change has the drawback that it may affect the FMO energies of the cyclopropane fragment and its interaction with the ethene function.

4 **5** **6**

In order to assign the structures of vinylcyclopropane radical cationic systems, we consider the frontier molecular orbital (FMO) of the cyclopropane unit and consequences for the interaction between the two moieties. MO calculations suggest that the vertical ionization of cyclopropane occurs from a degenerate pair of in-plane e' orbitals (**s**, **a**) resulting in a doubly degenerate ^{2}**E'** state;[14] first-order Jahn-Teller distortion leads to two non-degenerate electronic states, ^{2}**A$_1$** and ^{2}**B$_2$** (C_{2v} symmetry).[14] The ^{2}**A$_1$** component (orbital **s** singly occupied) relaxes to a "one-electron-bonded trimethylene" structure (type **A**) with one lengthened C–C bond. This structure type has been assigned to many cyclopropane radical cations, based on either CIDNP[2d,g,15] or low-temperature ESR spectra.[16]

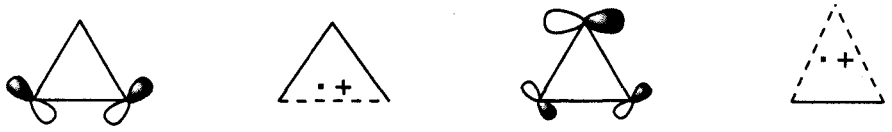

s **A** **a** **B**

The alternative ^{2}**B$_2$** component has a singly occupied antisymmetrical molecular orbital **a**. The resulting structure resembles a "π-complex" (type **B**) with two lengthened C–C bonds.[15] This structure type may be stabilized by substitution at a single carbon as in the parent vinylcyclopropane radical cation.[9] The substrates discussed here are 1,1,2-tri-substituted cyclopropanes; precedent[15,16] and ab-initio MO calculations[14f] suggest that this substitution pattern favors a structure of the "one-electron-bonded trimethylene" type (**A**).

Radical cations of the ^{2}**A$_1$** structure type pose the interesting question whether ring opening to a bifunctional trimethylene radical cation (**TM**) is possible, and how this putative species is related to the propene radical cation (**P**). These problems have been addressed previously by theoretical and experimental methods; the results reported here will be discussed in terms of the putative ring opening.

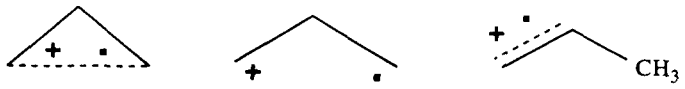

A TM P

Nuclear Spin Polarization

We will base the structures of the three vinylcyclopropane radical cations on (chemically induced) nuclear spin polarization (CIDNP) effects, which may be induced in radical ion pairs, when photo-induced (eq 1) electron transfer reactions (eq 2) are carried out in the probe of an NMR spectrometer.[2d] The resulting radical ion pairs undergo intersystem crossing (eq 3) followed by recombination of the singlet pairs (eq 4), or suffer separation by diffusion, generating "free" radical ions (eq 5). The competing processes (eq 3–5) give rise to a pattern of enhanced absorption or emission lines in the NMR spectrum. The polarization patterns are determined by four parameters, including sign and magnitude of the hyperfine coupling constants (hfc, A) of the nuclei in the radical cation, the relative magnitude of the g-factor of the intermediate (Δg), the initial spin multiplicity of the radical ion pair (which is dictated by the precursor spin multiplicity; μ) and the mode of product formation (ε).[17-20] CIDNP has been applied successfully to probe the structures of numerous radical cations.[2d,15]

Scheme 1

$$\mathrm{Chl} \xrightarrow{h\nu} {}^1\mathrm{Chl}^* \xrightarrow{ISC} {}^3\mathrm{Chl}^* \quad (1)$$

$$^3\mathrm{Chl}^* + \mathrm{D} \xrightarrow{ET} {}^3\overline{\mathrm{Chl}^{\bullet-}\ \mathrm{D}^{\bullet+}} \quad (2)$$

$$^3\overline{\mathrm{Chl}^{\bullet-}\ \mathrm{D}^{\bullet+}} \xrightarrow{ISC} {}^1\overline{\mathrm{Chl}^{\bullet-}\ \mathrm{D}^{\bullet+}} \quad (3)$$

$$^1\overline{\mathrm{Chl}^{\bullet-}\ \mathrm{D}^{\bullet+}} \xrightarrow{BET} \mathrm{Chl} + \mathrm{D} \quad (4)$$

$$^3\overline{\mathrm{Chl}^{\bullet-}\ \mathrm{D}^{\bullet+}} \xrightarrow{DIFF} {}^2\mathrm{Chl}^{\bullet-} + {}^2\mathrm{D}^{\bullet+} \quad (5)$$

EXPERIMENTAL

CIDNP experiments were carried out by irradiation of the sample in the probe of a Bruker AF 250 (250 MHz) NMR spectrometer equipped with a fused silica light-pipe. The collimated beam of a Hanovia 1000W high pressure Hg-Xe lamp was passed through a water filter, an aqueous $CuSO_4$ filter solution and, last, through a $\lambda > 370$ nm cut-off filter.

Materials and Solvents. The electron acceptor, 2,3,5,6–tetrachlorobenzoquinone (Aldrich, 98%), was recrystallized before use. Sabinene (**1**; Aldrich) was used as received; α- (**2**) and β-thujene (**3**) were prepared from thujone (Aldrich) and separated by GC as described previously.[6,21] The deuterated solvent, acetone-d_6 (Aldrich), was used as received.

Isolation of Products. The reaction products were isolated by column chromatographic procedures, on columns of 1.2 cm ID, packed with ~ 10 – 15-cm of silica gel (VWR Scientific, 230 – 400 mesh) and eluted with solvent gradients, usually from light petroleum ether (B.P. < 65°C) to mixtures with ethyl acetate.

Characterization of Products. All reaction products were previously characterized; they were identified by their GC retention times, MS, and NMR data. ^{1}H NMR spectra were recorded on Varian XL-400 or a Varian Gemini-200 spectrometer, ^{13}C spectra on the Gemini spectrometer, operating at 50.3 MHz.

RESULTS and DISCUSSION

Irradiation of chloranil in the presence of the three donors led to strong CIDNP effects for the respective donor molecules as well as for some rearrangement products. These results offer insight into the spin density distribution of the corresponding radical cations and elucidate some of their reactions. The effects are ascribed to the reaction sequence (eq 1-4) which regenerates the donor. Given the short singlet lifetime of chloranil ($\mu > 0$) and the large g factor of tetrachlorosemiquinone ($g = 2.0050$)[22] compared to those of typical hydrocarbon radical ions ($g \sim 2.0027$; $\Delta g < 0$),[22] enhanced absorption or emission signals for the regenerated donor ($\varepsilon > 0$) indicate negative or positive hfcs for the corresponding nuclei of the radical cation, respectively.

Sabinene Radical Cation. The CIDNP spectrum observed during the electron transfer reaction of sabinene (Fig. 1) shows strongly enhanced absorption signals for H_5 (1.59 ppm) and for the exo-methylene protons (4.55 and 4.75 ppm); these results suggest significant positive spin density on C_5 and on the terminal methylene carbon, C_{10}. Emission signals for the isopropyl methine proton (1.50 ppm; H_7), the geminal cyclopropane protons (0.63 ppm, H_6), and the geminal protons attached to C_2 (1.70 ppm), suggest substantial spin density on an adjacent carbon. The emission of the geminal cyclopropane protons (H_6) can be ascribed to the spin density at C_5; the polarization of H_7 and H_2 requires positive spin density on the quaternary cyclopropane carbon, C_1. Thus, the CIDNP results support delocalization of the electron spin between the olefinic π-system and the internal cyclopropane bond; they are compatible with a vinylcyclopropane radical cation, $\mathbf{1}^{\bullet+}$, with one weakened cyclopropane bond (Scheme 2). The lack of polarization for the allylic protons at C_3 reflects their attachment at or near the node, between the two centers of spin density, C_{10} and C_5.

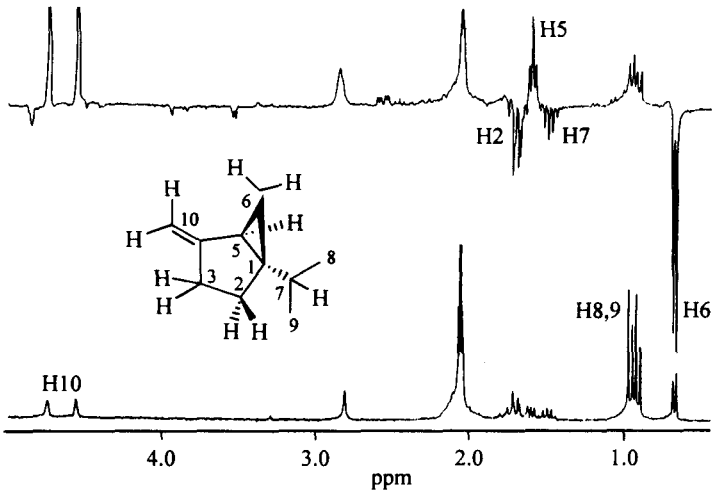

Figure 1. ^{1}H CIDNP spectrum (250 MHz; top) observed during irradiation of chloranil with sabinene (**1**) in acetone-d_6 and dark spectrum (bottom). Assignments are based on the 2-D ^{1}H-^{1}H COSY spectrum.

The CIDNP spectrum (Fig. 1) also shows three weak emission signals (δ 4.85, 3.95, 3.52 ppm) and an absorption multiplet (δ 2.6 ppm). The signal at δ 4.85 lies in the range typical for a terminal olefinic methylene function, suggesting ring-opened products such as β-phellandrene (**7**) or β-terpinene (**8**), which are formed by thermal isomerization of **1**.[23] However, the observed chemical shift does not match the spectra of **7** and **8**.

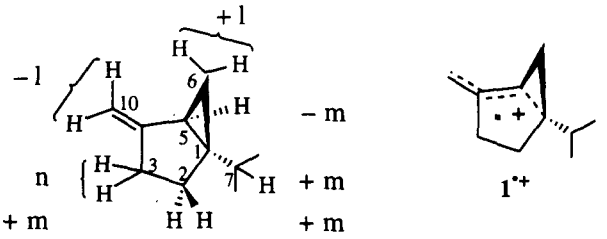

Scheme 2. Hyperfine coupling pattern of $1^{\bullet+}$ based on CIDNP and suggested delocalized structure.

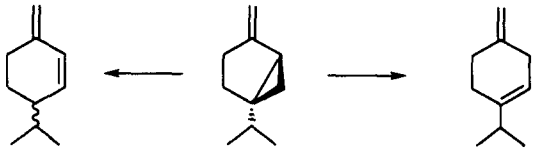

7 1 8

The strongly deshielded signals at δ 3.95 and 3.52 ppm are typical for protons attached to alkoxy substituted carbons. Therefore, the enhanced signals are tentatively assigned to an adduct between a rearranged radical cation and the quinone radical anion. The formation of such adducts has precedence. For example, several quinone adducts of different structure types were formed in the photoreactions between chloranil as sensitizer and 2,2-diphenyl-1-methylenecyclopropane[24] or 1,1-dimethylindene.[25] Similarly, three benzoquinone adducts were obtained from norbornadiene.[26]

In this context it is of interest that the photoreaction with chloranil partially converts **1** to **2** (~20%); the rearranged hydrocarbon shows no CIDNP effects. According to the mass spectrum, 40% of the newly generated **2** has incorporated one deuterium, most likely by abstraction from the solvent, acetone-d_6. The formation of **2** is rationalized via proton transfer from $\mathbf{1}^{\bullet+}$ to $\mathbf{Chl}^{\bullet-}$; the resulting allylic free radical, $\mathbf{9}^{\bullet}$, may abstract deuterium from the solvent, generating **2** with deuterium incorporation. Alternatively, $\mathbf{9}^{\bullet}$ may react by hydrogen atom transfer from $^{\bullet}$**Chl**–H, regenerating the unchanged educt.

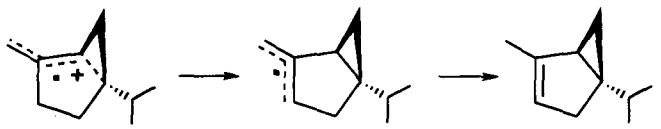

$1^{\bullet+}$ $9^{\bullet}$ 2

The protonation of quinone radical anions has ample precedent,[27-30] as does the hydrogen transfer from $^{\bullet}$**Chl**–H.[31] Likewise, deprotonation of radical cations is well established.[4i,6,32] The failure to observe CIDNP effects for **2** in this experiment is ascribed to the comparatively slow rate of hydrogen atom transfer. In contrast to electron transfer in radical ion pairs, hydrogen atom transfer to neutral radicals may be considerably slower than nuclear spin lattice relaxation in free radicals ($^2T_{1,n} \sim 10^{-6}$ s). Particularly, if **2** is formed after cage escape of $\mathbf{9}^{\bullet}$, any polarization of these radical(s) may be lost due to nuclear relaxation.

α-Thujene Radical Cation. The CIDNP spectrum observed during the electron transfer reaction between chloranil and α-thujene shows characteristic enhanced signals for the substrate (Fig. 2). Strongly

enhanced absorption for the olefinic resonance (δ 4.95 ppm; H_3) and strong emission for the geminal allylic protons (δ 2.15, 2.28 ppm; H_2) support significant spin density on C_3; similarly, the emission observed for the allylic methyl signal (δ 1.75 ppm; H_{10}) supports substantial spin density on C_4. Thus, the α-thujene radical cation ($2^{\bullet+}$) bears significant spin density on both olefinic carbons. Only limited spin density is indicated for the cyclopropane carbons. The tertiary allylic proton (δ 1.44 ppm; H_5) and the isopropyl methine multiplet (δ 1.47 ppm; H_7) show negligible polarization. However, the weak emission of $H_{6,anti}$ (0.75 ppm) and the weak *net* emission of $H_{6,syn}$ (0.0 ppm) require some spin density on at least one adjacent carbon, i.e., the tertiary (C_5) and/or quaternary cyclopropane carbons (C_1).

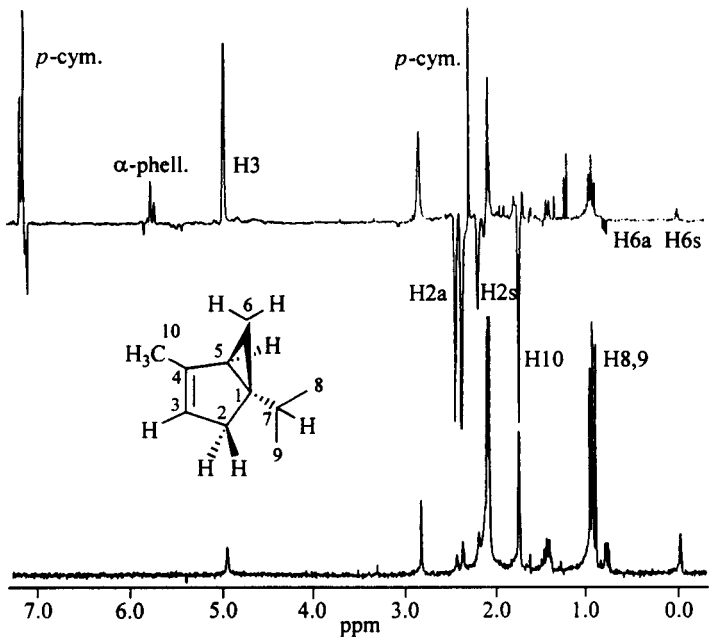

Figure 2. ^1H CIDNP spectrum (250 MHz; top) observed during irradiation of chloranil with α-thujene (**2**) in acetone-d_6 and dark spectrum (bottom). Assignments are based on 2-D ^1H-COSY and NOE spectra.

Because the CIDNP effects of the cyclopropane protons are weak, they might arise by alternative polarization mechanisms, such as cross relaxation[33-35] between these protons and more strongly polarized nuclei, e.g., H_2, H_3, or H_{10}. However, we find no evidence to support this suggestion. Effective cross relaxation requires that the interacting nuclei have either strong scalar spin-spin coupling or spatial proximity.

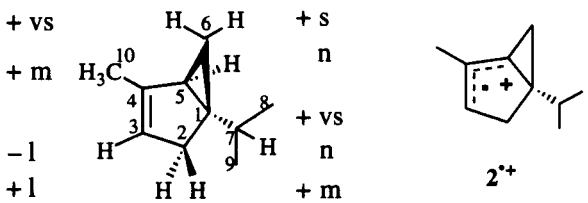

Scheme 3. Hyperfine coupling pattern for $2^{\bullet+}$ based on CIDNP effects and suggested structure.

The three cyclopropane protons of **2** have no appreciable J coupling with the olefinic or allylic protons, nor do NOE difference spectra show significant interactions between these protons. The observed CIDNP effects support the delocalization of spin and charge onto the cyclopropane fragments, mostly on the tertiary allylic cyclopropane carbon. This finding suggests for **2**$^{\bullet+}$ a structure with a weakened internal cyclopropane bond (Scheme 3).

Interestingly, the pairs of geminal protons at C_2 and C_6 have somewhat different hfcs. The divergent hfcs of the allylic protons ($H_{2syn,anti}$) can be explained by different orientations with respect to the olefinic p orbital. Molecular models of α-thujene suggest that the C_2–H_{2anti} bond of the preferred conformer is nearly parallel to the olefinic p-orbital whereas the C_2–H_{2syn} bond lies in a plane close to the cyclopentene ring plane; therefore, H_{2anti} has a much stronger hfc. The allylic protons of bicyclo[3.1.0]hex-2-ene, **5**,[10] have similarly divergent CIDNP effects. For **5**$^{\bullet+}$, the effects were reproduced well by ab-initio calculations at appropriate levels of theory, as discussed below. The weak, slightly different hfcs suggested for the two geminal cyclopropane protons ($H_{6syn,anti}$) may be due to competiting π,σ polarization and π,σ delocalization (hyperconjugation).[36] Analogous CIDNP effects were observed for the corresponding ^{1}H nuclei of **5**;[10] these effects are also reproduced by our *ab initio* calculations.

The reaction of **2** with excited chloranil also leads to two polarized products, *p*-cymene (**10**) and α-phellandrene (**11**). One aromatic resonance of **10** (δ 7.07 ppm; H_3) shows emission, whereas the second aromatic resonance (H_2; δ 7.13 ppm) and the benzylic methyl signals (δ 2.3 ppm) show enhanced absorption. These signal directions are opposite to the corresponding signals of **2** (H_3, H_5, absorption; H_2, H_6, H_7, H_{10}, emission). All three olefinic resonances of **11** are polarized; H_4 (δ 5.72 ppm) shows absorption whereas H_1 (δ 5.45 ppm) and H_3 (δ 5.78 ppm) show weak emission. Again, these signal directions are opposite to the corresponding resonances of **2**.

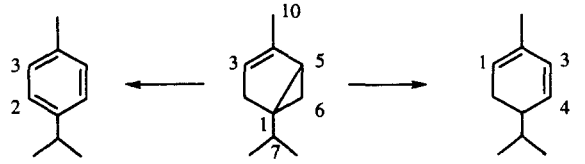

10 **2** **11**

Because of the characteristic relationship between the polarization patterns of **10** and **11** to the hfc pattern of **2**$^{\bullet+}$, we conclude that the polarization is induced in **2**$^{\bullet+}$, and that **10** and **11** are formed by a mechanism different from that regenerating **2**. We suggest that **10** is formed via deprotonation of **2**$^{\bullet+}$ (i.e., proton transfer from **2**$^{\bullet+}$ to **Chl**$^{\bullet-}$), followed by hydrogen atom transfer from the resulting **13**$^{\bullet}$ to the semiquinone radical, **Chl**$^{\bullet}$–H. The deprotonation is driven by release of ring strain and increased electron delocalization, whereas the hydrogen atom transfer is favored by aromatization.

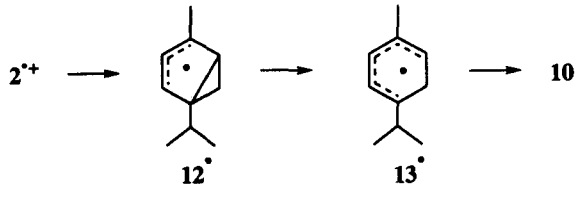

12$^{\bullet}$ **13**$^{\bullet}$

According to this mechanism, **10** is as an "in-cage" product; yet, its signal direction is that of an "escape" product. This seeming discrepancy can be resolved by invoking an unusual spin-sorting principle. The key to the spin sorting lies in the different rates of the competing reactions forming **2** and **10**. Back electron transfer, regenerating **2**, is electron spin dependent and fast. On the other hand, proton transfer, which converts the radical ion pair, **2**$^{\bullet+}$ ···· **Chl**$^{\bullet-}$, to a pair of neutral radicals, **13**$^{\bullet}$ ···· $^{\bullet}$**Chl**–H, is electron spin independent; however, the hydrogen atom transfer (disproportionation) of the secondary pair is slow.

In general, spin sorting is achieved by the competition between back electron transfer and any electron spin independent process, including the proton transfer step generating **13**$^{\bullet}$. Nuclear spin states allowing fast intersystem crossing predominate in regenerated **2**; those retarding intersystem crossing accumulate in secondary products, including recombination products such as **10**. The proposed spin-sorting principle is unusual, but not without precedent.[37,38] It was invoked originally to explain CIDNP effects observed during the photolysis of dibenzyl ketone in micelles where a "conventional" cage escape reaction does not exist. Instead, the spin sorting is accomplished by a competition between an early recombination of the geminate pair and a delayed recombination of a secondary pair.[37]

Although the CIDNP data do not reveal the detailed mechanism by which **11** is generated, this mechanism was recently established by studying a mono-deuterium labeled sample. The fate of the isotopic label revealed competing [1.3] and homo-[1,5] sigmatropic shifts.[6] In this system, spin sorting is achieved by the competition between back electron transfer and the slower, electron spin independent sigmatropic shifts, generating the secondary radical ion pair, **11**$^{\bullet+}$ ···· **Chl**$^{\bullet-}$, from the primary pair, **2**$^{\bullet+}$ ···· **Chl**$^{\bullet-}$.

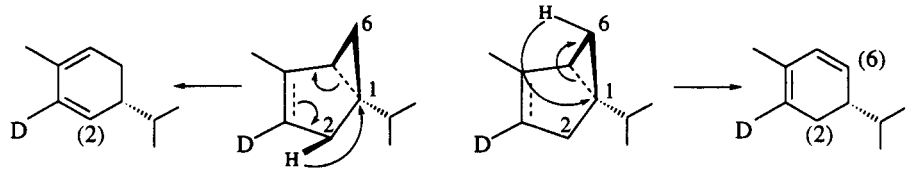

(–)–**11**-d_1 (–)–**2**-3-d_1 (–)–**2**-3-d_1 (+)–**11**-d_1

In summary, the α-thujene radical cation, **2**$^{\bullet+}$, bears significant spin density on both olefinic carbons and some spin density on the tertiary cyclopropane carbon, but negligible spin density on the other cyclopropane carbons. The fact that the pairs of geminal protons ($H_{2syn,anti}$ and $H_{6syn,anti}$) show non-equivalent hfcs is incompatible with a ring-opened radical cation, in which these nuclei would be related by symmetry. Instead, the CIDNP spectrum suggests a ring-closed structure (**2**$^{\bullet+}$) with one weakened cyclopropane bond; clearly, the radical cation retains the steric integrity of the parent molecule.

β-Thujene Radical Cation. The CIDNP spectrum observed during the photoreaction of chloranil with β-thujene (**3**) features signals of polarized, **3**, and of an aromatization product, **10**, in addition to weak unidentified signals (Fig. 3); the polarization is slightly weaker than those of **1** and **2**. Enhanced absorption for one olefinic signal (5.34 ppm; H_3) and emission for the tertiary allylic proton (2.42 ppm; H_4) suggest positive spin density on the olefinic C_3. Weak emission for the isopropyl methine multiplet (1.41 ppm, H_7) supports spin density at the quaternary cyclopropane carbon, C_1. The second olefinic proton (5.81 ppm; H_2) is not enhanced, indicating negligible spin density at C_2. This result suggests that H_2 lies at or near a node, between the two centers of spin density, C_3 and C_1. Of the cyclopropane protons, only H_{6anti} (0.75 ppm) shows weak

emission. This effect requires spin density at an adjacent carbon, either C_1 or C_5; the emission of the isopropyl methine multiplet (δ 1.47 ppm; H_7) supports spin density on the quaternary cyclopropane carbon (C_1). Thus, the CIDNP effects observed for **3** suggest that its radical cation has spin density on C_3 and C_1. This spin density distribution allows for a somewhat weakened internal cyclopropane bond. Nevertheless, the steric integrity of β-thujene is conserved in its (ring-closed) radical cation, **3**$^{\bullet+}$ (Scheme 4). This assignment is borne out by *ab initio* calculations on the truncated radical cation, **5**$^{\bullet+}$,[10] or its methyl derivative, **6**$^{\bullet+}$.

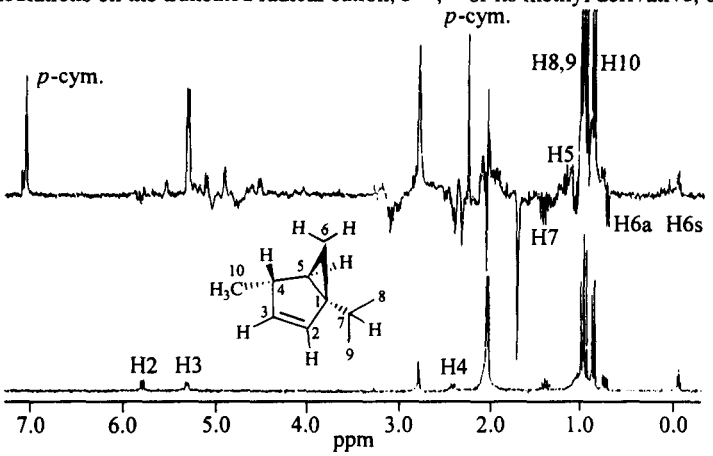

Figure 3. ^{1}H CIDNP spectrum (250 MHz; top) observed during irradiation of chloranil with β-thujene (**3**) in acetone-d_6 and dark spectrum (bottom; assignments are based on 2-D ^{1}H-COSY and NOE spectra).

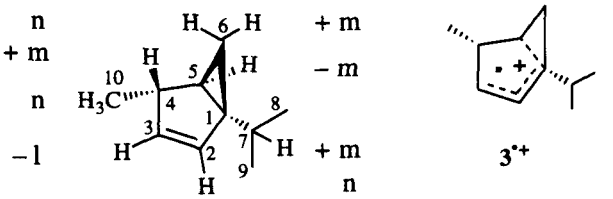

Scheme 4. Hyperfine coupling pattern of **3**$^{\bullet+}$ based on CIDNP effects and suggested delocalized structure.

MO Calculations on Substituted Vinylcyclopropane Radical Cations

Our CIDNP results show that the three vinylcyclopropane radical cations (**1**$^{\bullet+}$ – **3**$^{\bullet+}$) have major spin density on the olefinic β carbon and the allylic cyclopropane carbon. The species differ in the spin density distribution on the other ring carbons. The structure of **1**$^{\bullet+}$ appears to come close to prototype **A**, derived from the symmetrical (*S*) SOMO of cyclopropane radical cation. The electron spin densities of **2**$^{\bullet+}$ and **3**$^{\bullet+}$ are delocalized noticeably only onto one cyclopropane carbon; these radical cations may have some contribution due to the antisymmetrical cyclopropane HOMO (*A*), i.e., they may share elements of prototypes **A** and **B**.

The structures of some vinylcyclopropane radical cations can be elucidated by considering the frontier molecular orbital (FMO) interactions between the cyclopropane and alkene moieties. A qualitative analysis of this interaction can be based on the principles of perturbational molecular orbital (PMO) theory.[39,40] The substrates are dissected into fragments and the potential interactions of the component FMOs are considered.

The strength of the fragment perturbation depends on factors such as: the relative energy of the interacting orbitals; the FMO symmetry; the magnitude of the coefficients at the point(s) of union; and the orientation of the fragments relative to each other.[39] The closer the orbitals are in energy and the higher the extent of orbital overlap, the greater their mutual interaction.

The FMO energies of unsubstituted ethylene (10.5 eV)[41] and cyclopropane (10.6 eV)[42] appear closely matched; these functions may interact strongly, given a favorable orientation. Compared to its components, the first ionization potential of vinylcyclopropane (9.2 eV) is lowered significantly,[43] demonstrating strong interaction. However, an analysis of the three radical cation structures discussed here is complicated by several factors. First, the structures of $\mathbf{1}^{\bullet+}$ – $\mathbf{3}^{\bullet+}$ result from the perturbation of the ethylene (*E*) FMO by not one but any of three cyclopropane orbitals, which may be involved to different degrees. One FMO is formally derived from the antisymmetrical orbital, *A*, and has a significant orbital coefficient (~2/3)[44] at the allylic cyclopropane carbon. In addition, two FMOs formally derived from the "symmetrical" orbital, *S*, may be involved, with orbital coefficents on the carbons of either the internal (S_i) or a lateral cyclopropane bond (S_l).

The presence of methyl and isopropyl groups present additional difficulties. Alkyl substituents lower the ionization potentials of ethylene and cyclopropane derivatives by 0.5 – 0.8 eV per alkyl group, due to hyperconjugation. This interaction increases the FMO energies of the olefinic or cyclopropane moieties, affects the match between the component FMOs, and may change the prevailing structure by changing the nature of the cyclopropane FMO most closely matched with the *E* FMO. Finally, the center of the bent cyclopropane bonds lies ~ 20° outside the direct C–C connection,[45] and the orientations of the three cyclopropane orbitals relative to *E* may be subject to conformational changes. In view of these considerations, it is unlikely that the subtle differences between the three radical cations, $\mathbf{1}^{\bullet+}$ – $\mathbf{3}^{\bullet+}$, can be elucidated by qualitative arguments.

Therefore, we approached their structures by *ab initio* calculations[11] on three models: radical cation $\mathbf{4}^{\bullet+}$ is a simplified model for the *anti*-fused $\mathbf{1}^{\bullet+}$; $\mathbf{5}^{\bullet+}$ has the *syn*-orientation, like $\mathbf{2}^{\bullet+}$ and $\mathbf{3}^{\bullet+}$, but has no alkyl groups; finally, the methyl group gives $\mathbf{6}^{\bullet+}$ a quaternary cyclopropane carbon. These species were calculated with the GAUSSIAN 94 electronic structure programs,[12] using extended basis sets, including p-type polarization functions on carbon (6-31G*), and appropriate levels of electron correlation (MP2). Density functional theory methods were also applied (B3LYP). The simplified models, particularly the omission of the isopropyl group, were chosen to limit the significant computing resources required for the calculations, although this may alter the FMO energies of the cyclopropane fragments and affect the interaction with the ethene group.

Molecular structures were optimized at the unrestricted Hartree-Fock level with the 6-31G* basis set (UHF/6-31G*). The structures obtained in this way were further optimized including electron correlation contributions using Møller-Plesset perturbation theory through second order (MP2/6-31G*). In view of previous experience we expect this level of theory to be sufficient for the major structural features of these systems.[14f,46-48] Calculations at this level appear to provide reasonable geometries (although no experimental data are available to compare directly with the calculated results). The calculations also afford spin densities and hyperfine coupling constants; these can be compared with EPR or CIDNP results.

We have shown in several systems that second-order Møller-Plesset perturbation theory reproduces positive hfcs quite well; positive splittings arise from hyperconjugative interactions between magnetic nuclei and the unpaired electron spin; they are proportional to the calculated Fermi contact terms. Positive hfcs can be calculated within ± 10%. In contrast, negative hfcs are significantly overestimated at the MP2 level, often by

Table 1. Calculated Bond Lengths (Å) of Bridged Vinylcyclopropanes and Radical Cations

Bond	**4** MP2//MP2	$\mathbf{4}^{\bullet+}$ HF//HF	$\mathbf{4}^{\bullet+}$ B3LYP//B3LYP	$\mathbf{4}^{\bullet+}$ MP2//MP2
C1-C2	1.483	1.395	1.416	1.407
C1-C5	1.519	1.619	1.727	1.636
C1-C6	1.516	1.594	1.557	1.588
C2-C7	1.340	1.411	1.390	1.399
C5-C6	1.498	1.427	1.445	1.437
Bond	**5** MP2//MP2	$\mathbf{5}^{\bullet+}$ HF//HF	$\mathbf{5}^{\bullet+}$ B3LYP//B3LYP	$\mathbf{5}^{\bullet+}$ MP2//MP2
C1-C2	1.487	1.401	1.420	1.419
C1-C5	1.520	1.536	1.559	1.566
C1-C6	1.512	1.748	1.682	1.633
C2-C3	1.345	1.387	1.393	1.393
C5-C6	1.502	1.443	1.452	1.447
Bond	**6** MP2//MP2	$\mathbf{6}^{\bullet+}$ HF//HF	$\mathbf{6}^{\bullet+}$ B3LYP//B3LYP	$\mathbf{6}^{\bullet+}$ MP2//MP2
C1-C2	1.486	1.390	1.408	1.416
C1-C5	1.520	2.359	2.006	1.606
C1-C6	1.516	1.535	1.531	1.602
C2-C3	1.345	1.389	1.378	1.391
C5-C6	1.502	1.475	1.460	1.446

factors > 2.[14f,46-48] However, density functional theory has been reported to give satisfactory agreement with experimental results.[13] Accordingly, we have optimized the structures at both the MP2 and the B3LYP levels (6-31G* basis set) and carried out single point B3LYP population analyses for the spin densities (ρ) and hfcs. Both treatments yield similar results.

Our calculations for $\mathbf{4}^{\bullet+}$ show characteristic changes in bond lengths upon one-electron oxidation (Table 1). Three C–C bonds are lengthened, including the exo-methylene bond from 134.0 to 139.9 pm, the internal cyclopropane bond (C_1–C_5) from 151.9 to 163.6 pm, and the lateral (C_1–C_6) bond from 151.6 to 158.8 pm;

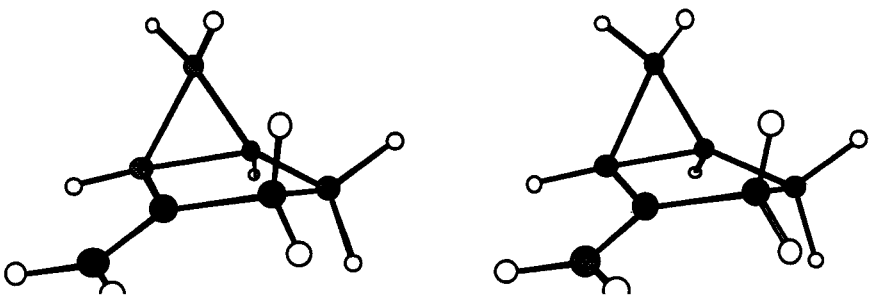

Table 2. Spin Density Distribution for Model Radical Cations $4^{\bullet+}$, $5^{\bullet+}$ and $6^{\bullet+}$

$4^{\bullet+}$	HF//HF	B3LYP//B3LYP	MP2//B3LYP	MP2//MP2
C1	0.168	0.240	0.209	0.191
C2	–0.092	-0.023	0.009	–0.113
C3	0.012	0.012	0.009	0.012
C4	–0.008	-0.009	–0.003	–0.010
C5	0.123	0.213	0.134	0.156
C6	0.106	0.062	0.100	0.091
C7	0.929	0.599	0.630	0.912
$5^{\bullet+}$	HF//HF	B3LYP//B3LYP	MP2//B3LYP	MP2//MP2
C1	0.319	0.209	0.202	0.195
C2	–0.262	0.084	0.091	–0.028
C3	0.830	0.486	0.511	0.788
C4	–0.058	–0.012	–0.015	–0.062
C5	–0.037	0.041	0.052	0.035
C6	0.426	0.243	0.203	0.247
$6^{\bullet+}$	HF//HF	B3LYP//B3LYP	MP2//B3LYP	MP2//MP2
C1	1.120	0.417	0.252	0.277
C2	–0.752	–0.114	0.059	–0.105
C3	1.123	0.532	0.526	0.825
C4	–0.108	–0.038	–0.019	–0.071
C5	0.017	0.335	0.090	0.111
C6	–0.108	–0.029	0.132	0.153
C7	–0.005	–0.017	0.017	0.007

two bonds are shortened, viz., the vinylic C_1–C_2 bond from 148.3 to 140.7 pm, and the lateral (C_5–C_6) bond from 149.8 to 143.7 pm. The spin density distribution calculated for **4**$^{\bullet+}$ at the (B3LYP/6-31G*//MP2/6-31G*) level reflects these changes, $\rho_7 = 0.63$, $\rho_1 = 0.209$, $\rho_5 = 0.134$, $\rho_6 = 0.10$ (Table 2). Finally, the calculations provide a set of hyperfine coupling constants; the large negative hfcs of the exo-methylene protons, H_7, and the positive hfcs of H_{3s}, H_{4s}, and H_{6s} are most noticeable (Table 3). The truncated model, **4**$^{\bullet+}$, appears to be a adequate model for **1**$^{\bullet+}$; the results confirm the exo-methylene carbon as the major center of spin density and indicate some delocalization into the ring, particularly onto C_1. The calculations nicely reproduce the major trends of the CIDNP results for **1**$^{\bullet+}$, especially the major polarization of H_{10} and H_{6s}, including the noticeable difference between H_{6s} and H_{6a}. Concerning **4**$^{\bullet+}$, one can safely predict that addition of an isopropyl group at C_5 will divert some spin (and charge) density onto C_5, most likely at the expense of C_6. One noticeable difference between experiment (CIDNP of **1**) and calculations (hfcs of **4**$^{\bullet+}$) lie in the significant hfcs predicted for $H_{3s,a}$. This discrepancy may be due to a steric effect of the isopropyl group.

Table 3: Comparison of CIDNP Effects[a] with Calculated Hyperfine Coupling Constants

$1^{\bullet+}$		$4^{\bullet+}$				
Proton	CIDNP	Proton	Calculated hyperfine coupling constants			
			HF//HF	B3LYP//B3LYP	B3LYP//MP2	MP2//MP2
H5	+m	H1	–6.0	–6.2	–5.0	–7.2
H3s	n	H3s	1.0	4.5	6.5	0.6
H3a	n	H3a	1.0	3.6	3.9	0.7
H2s	–m	H4s	2.8	11.1	7.0	3.6
H2a	–m	H4a	0.6	2.9	1.6	1.0
		H5	3.0	–1.2	3.8	1.4
H6s	–s	H6s	2.6	13.5	7.1	4.4
H6a	–s	H6a	0.9	3.6	2.8	2.0
H10s	+s	H7s	–35.4	–14.2	–15.2	–35.0
H10a	+s	H7a	–35.8	–14.3	–15.4	–35.3
H7	–m					
H8[b]	n					
H9[b]	n					

a) + enhanced absorption; – enhanced emission; s = strong; m = medium; w = weak; n = negligible. For the systems discussed here emission indicates a positive hfc, whereas absorption indicates a negative hfc.

b) averaged value of the methyl proton hfc's.

Sabinene is numbered according to the terpene nomenclature convention: Nomenclature Committee of the Division of Organic Chemistry, ACS *Systems of Nomenclature for Terpene Hydrocarbons. Acyclics, Monocyclics, Bicyclics, Advances in Chemistry Series No. 14*, ACS: Washington, D.C., 1955

The calculations for $\mathbf{5}^{\bullet+}$ also show characteristic changes upon oxidation (Table 1). Three bonds are lengthened, including the double bond (134.5 to 139.3 pm), the internal cyclopropane bond (C_1–C_5; 152.0 to 155.9 pm), and one lateral bond (C_1–C_6; 151.2 to 163.3 pm); the vinylic C_1–C_2 bond (148.7 to 141.9 pm), and the lateral bond (C_5–C_6; 150.2 to 144.7 pm) are shortened. The calculated spin densities, $\rho_3 = 0.511$, $\rho_1 = 0.202$, $\rho_5 = 0.052$, and $\rho_6 = 0.203$ (B3LYP/6-31G*//MP2/6-31G*; Table 2), reflect these changes. These structural changes differ from those observed for the oxidation of **4** especially in the greater spin density at the secondary cyclopropane carbon and in the greater participation of two cyclopropane bonds in delocalizing spin (and charge). One significant negative hfc is calculated for H_3 (–13.5 G); of the positive hfcs the difference between H_{4a} (38.4 G) and H_{4s} (10.2 G) is most noticeable (Table 4). The calculated spin density distribution and hfcs nicely reproduce the structure derived for radical ion $\mathbf{5}^{\bullet+}$ from CIDNP results,[10] especially the major polarization of H_4 and H_3 and including the difference between H_{4a} and H_{4s}.

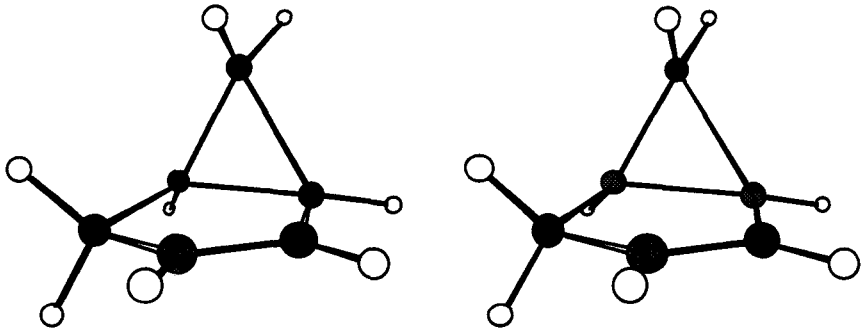

Figure 5. Stereoview of radical cation $\mathbf{5}^{\bullet+}$ fully optimized at the MP2 level of theory (6-31G* basis set).

A comparison of $\mathbf{5}^{\bullet+}$ with the structures assigned to $\mathbf{2}^{\bullet+}$ and $\mathbf{3}^{\bullet+}$ based on the CIDNP results indicates agreement in the major features but also points to shortcomings of the truncated model. The results confirm the alkene function as the major center of spin density and reproduce the major polarization observed for **2** and **3**, including the absorption of the olefinic protons, H_3. The calculations also support delocalization into the cyclopropane ring, mostly onto C_1. However, the omission of the isopropyl group may alter the spin density distribution, particularly with respect to $\mathbf{2}^{\bullet+}$. Inclusion of such a function should favor delocalization into the internal cyclopropane bond, diverting spin density from the secondary to the quaternary carbon. These considerations suggest the radical cation of 5-methylbicyclo[3.1.0]hex-2-ene, **6**, as a more appropriate model.

Introduction of the methyl group does not appreciably change the bond lengths of the neutral molecule relative to **5** (Table 1) but causes noticeable changes for the radical cation, $\mathbf{6}^{\bullet+}$. The internal cyclopropane bond is lengthened (C1–C5, 156.6 to 160.6 pm) while the lateral one is shortened (C1–C6, 163.3 to 160.2 pm). yielding bonds of nearly equal length. Corresponding changes are observed for the spin density distribution (B3LYP/6-31G*//MP2/6-31G*): the minor spin densities at C5 ($\rho 5 = 0.09$; +75%) and C1 ($\rho 1 = 0.25$; +25%) increase at the expense of those at C6 ($\rho 6 = 0.13$; –35%) and C2 ($\rho 2 = 0.06$; –35%) (Table 2). However, the principal spin density at C3 ($\rho 3 = 0.526$) remains unchanged. Thus, the alkyl substituent at C5 changes the radical cation structure from delocalization into a single cyclopropane bond (C1-C6) towards participation of the C1-C5 bond. The subtle changes in bond lengths and spin densities cause modest changes in the hfc's; notably, the geminal cyclopropane hfc's are in better agreement with the polarization observed of $\mathbf{2}^{\bullet+}$ and $\mathbf{3}^{\bullet+}$ (negligible

Table 4: Comparison of CIDNP Effects[a] with Calculated Hyperfine Coupling Constants

$2^{\bullet+}$		$3^{\bullet+}$		$5^{\bullet+}$						$6^{\bullet+}$				
						Calculated hyperfine coupling constants					Calculated hyperfine coupling constants			
Proton	CIDNP	Proton	CIDNP	Proton	CIDNP	HF/ /HF	B3LYP/ /B3LYP	B3LYP/ /MP2	MP2/ /MP2	Proton	HF/ /HF	B3LYP/ /B3LYP	B3LYP/ /MP2	MP2/ /MP2
H5	n			H1	+w	–8.2	–0.8	–0.8	–3.5	H1	–39.0	–9.8	–3.5	–8.2
		H2	n	H2	+w	8.6	–2.3	–1.8	0.2	H2	24.1	4.4	0.2	3.8
H3	+s	H3	+s	H3	+s	–29.8	–12.0	–13.5	–29.4	H3	–39.0	–11.9	–13.8	–30.6
H2s	–m	H4s	–m	H4s	–m	11.3	10.5	10.2	12.2	H4s	11.3	2.2	8.7	12.4
H2a	–s			H4a	–s	32.0	37.8	38.4	35.6	H4a	29.2	13.9	32.7	32.4
		H5	–m	H5	–s	19.5	16.4	14.8	11.4					
H6s	–w	H6s	n	H6s	+m	–15.4	–4.4	–3.5	–7.6	H6s	34.0	24.2	1.3	1.9
H6a	–w	H6a	–m	H6a	+w	–11.9	–1.5	1.1	–2.2	H6a	7.1	3.7	3.4	–0.9
H7[b]	n	H7[b]	–m							Me[b]	0.0	12.0	4.9	3.2
H8	n	H8	n											
H9[b]	n	H9[b]	n											
H10[b]	–m	H10[b]	n											

a) + enhanced absorption; – enhanced emission; s = strong; m = medium; w = weak; n = negligible. For the systems discussed here emission indicates a positive hfc, whereas absorption indicates a negative hfc.

b) averaged value of the methyl proton hfc's.

The thujenes are numbered according to the terpene nomenclature convention: Nomenclature Committee of the Division of Organic Chemistry, ACS *Systems of Nomenclature for Terpene Hydrocarbons. Acyclics, Monocyclics, Bicyclics, Advances in Chemistry Series No. 14*, ACS: Washington, D.C., 1955

to small emission; Table 4) Thus, alkyl substitution at C5 causes increased participation of the C1-C5 bond, diverting spin density from C6 to C5.

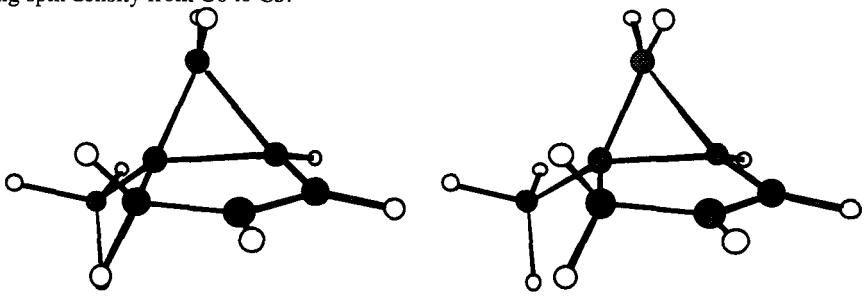

Figure 6. Stereoview of radical cation $\mathbf{6}^{\bullet+}$ fully optimized at the MP2 level of theory (6-31G* basis set).

Structure–Reactivity Relationship

Given the structures of $\mathbf{1}^{\bullet+}$ – $\mathbf{3}^{\bullet+}$, it is of interest whether their reactivities show an unambiguous relationship with structural features, such as the spin and charge density distribution. Radical cations undergo a wide range of reactions; their capture by nucleophiles has attracted particular attention. Here, we discuss briefly the nature (i.e., structure, stereochemistry, and chirality) of the "products" formed by nucleophilic capture in the light of the radical cation stuctures. We consider factors such as: the distribution of spin and charge in the radical cations (educts); the spin density distribution in the resulting free radicals (products); the extent of conjugation in educts and products; steric factors determining the approach of the nucleophile; stereoelectronic effects on structure or reaction; and the release of ring strain upon forming the product. It is also of interest to compare the radical cation reactions with those of their neutral diamagnetic precursors.

In 5-M methanol, $\mathbf{1}^{\bullet+}$ – $\mathbf{3}^{\bullet+}$ are captured by nucleophilic attack at a cyclopropane carbon; $\mathbf{1}^{\bullet+}$ and $\mathbf{2}^{\bullet+}$ yield $\mathbf{14}^{\bullet}$ and $\mathbf{15}^{\bullet}$, respectively, by exclusive capture at the highly hindered quaternary carbons; $\mathbf{3}^{\bullet+}$ forms $\mathbf{16}^{\bullet}$ by predominant attack at the 3° center, and $\mathbf{17}^{\bullet}$ by less efficient attack at the 2° carbon. In competition with capture by methanol, radical cations $\mathbf{1}^{\bullet+}$ and $\mathbf{2}^{\bullet+}$ react by [1,3]- and homo-[1,5]-sigmatropic shifts. Although $\mathbf{2}^{\bullet+}$ and $\mathbf{3}^{\bullet+}$ have the appropriate stereochemistry, neither undergoes a vinylcyclopropane rearrangement. The observed reactions exclude two factors: nucleophilic attack cannot be limited to centers of major spin density, since the reaction occurs predominantly on carbons with minor spin densities; steric hindrance is ruled out as a major factor, since $\mathbf{1}^{\bullet+}$ and $\mathbf{2}^{\bullet+}$ are captured at 4° carbons. The regiochemistry of attack supports relief of ring strain and formation of delocalized (allyl) π-systems as significant factors; both nucleophilic capture and hydrogen shifts fully release the inherent ring strain, forming conjugated delocalized free radicals. Interestingly, although the relief of ring strain plays a major role in the course of their reactions, the radical cations maintain a sufficient degree of bonding (and strain) in the cyclopropane function to conserve its stereochemical integrity.

The rate of nucleophilic capture is moderate; thus, the capture of 1,1-diphenyl-2,2-dimethylcyclopropane radical cation by methanol has a rate constant, $k \sim 3\times10^8$ $M^{-1}s^{-1}$.[4f] The slower than diffusion controlled rate is consistent with a selective capture and with the competing sigmatropic shifts, forming $\mathbf{7}^{\bullet+}$ from $\mathbf{1}^{\bullet+}$ and $\mathbf{11}^{\bullet+}$ from $\mathbf{2}^{\bullet+}$, respectively. In the light of this competition, it is significant that $\mathbf{3}^{\bullet+}$ forms products $\mathbf{16}^{\bullet}$ and $\mathbf{17}^{\bullet}$ by nucleophilic capture without competition from sigmatropic shifts. The failure of $\mathbf{3}^{\bullet+}$ to react by sigmatropic shift may elucidate the role of steric factors. The transition states for the capture of $\mathbf{3}^{\bullet+}$ involve less

hindered (2° or 3°) carbons than do those for the capture of $\mathbf{1}^{\bullet+}$ and $\mathbf{2}^{\bullet+}$. Reduced crowding renders the capture of $\mathbf{3}^{\bullet+}$ sufficiently fast to suppress hydrogen migration. This argument supports a definite, though minor role of steric hindrance in the nucleophilic capture of radical cations.

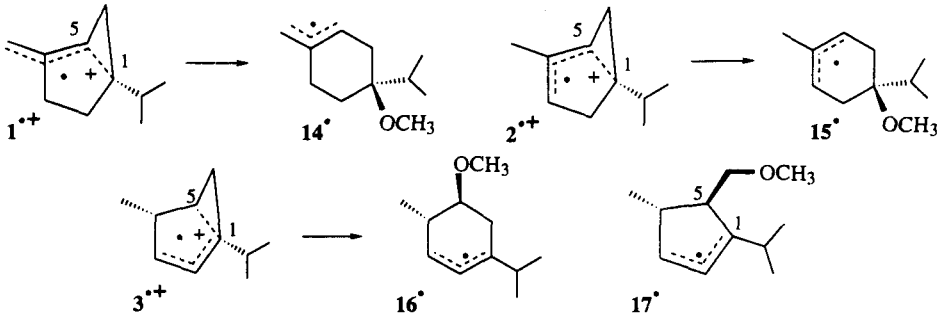

Concerning stereoelectronic effects, we consider effects such as those invoked to explain the attack at the 2° center of benzobicyclo[3.1.0]hex-2-ene.[4a] The CIDNP results for **5**[10] and the *ab initio* calculations reported here support this effect. Stereoelectronic effects may be caused by a favorable alignment of a cyclopropane Walsh orbital with the alkene p orbital; they may favor conjugation with the less highly substituted lateral cyclopropane bond, thus directing attack to C_6. The involvement of stereoelectronic effects can be evaluated by considering the dihedral angles between the cyclopropane and alkene orbitals (or between the alkene and cyclopropane bonds). For model ion $\mathbf{4}^{\bullet+}$, the dihedral angle, C7-C2-C1-C5, is −159°, corresponding to an orbital angle of ~35°. This does not allow a favorable overlap with the laternal (C1-C6) bond; neither the spin density on C6 nor the reactivity of $\mathbf{1}^{\bullet+}$ suggest a noticeable stereoelectronic effect. The model radical cations, $\mathbf{5}^{\bullet+}$ and $\mathbf{6}^{\bullet+}$, on the other hand, have dihedral angles, C3-C2-C1-C5, of −1.1° and −5.2°, respectively, corresponding to orbital angles of ~15° and 20°. For $\mathbf{5}^{\bullet+}$, the modest spin density at C6 supports a modest stereoelectronic effect; this is apparently borne out by the minor product resulting from nucleophilic attack on $\mathbf{3}^{\bullet+}$. In summary, the reactivity of radical cations, $\mathbf{1}^{\bullet+}$ – $\mathbf{3}^{\bullet+}$, is determined by relief of ring strain and formation of a delocalized π-system with lesser contributions from steric and stereoelectronic effects. Additional attempts to probe more significant stereoelectronic effects by CIDNP and ab-initio calculations are in progress.

In conclusion, it is of interest to compare thermal rearrangements of appropriate vinylcyclopropane derivatives with those of their neutral diamagnetic parents. Vinylcyclopropane derivatives rearrange by valence isomerization to cyclopentene systems, including the degenerate rearrangement of **2**,[21] or by homo-[1,5] sigmatropic shifts.[49] Although some 1-phenyl-2-vinylcyclopropane radical cations reportedly rearrange to cyclopentenes, this rearrangement is not observed for $\mathbf{2}^{\bullet+}$ or $\mathbf{3}^{\bullet+}$. On the other hand, the sigmatropic shifts of $\mathbf{1}^{\bullet+}$ and $\mathbf{2}^{\bullet+}$ are without precedent in the diamagnetic parent system. Although (–)-**2**-3-d_1 undergoes a homo-[1,5] sigmatropic shift to (–)-**7**-3-d_1, as does the neutral prototype, closer inspection reveals that the two pathways are entirely different. In fact, no homo-[1,5] sigmatropic shift was found in the thermal reorganization of **2**, which has been studied in significant detail.[21] The recognition that radical cations and their neutral diamagnetic precursors may react by significantly different pathways is noteworthy. It illustrates that the corresponding potential energy surfaces differ not only in degree but, occasionally, in principle. The vinylcyclopropane derivatives discussed here are salient examples for such divergence.

Acknowledgement

Financial support of this work by the National Science Foundation by grant NSF CHE-9414271 is gratefully acknowledged. This paper is dedicated, on the occasion of his 80th birthday, to Professor William von Eggers Doering. In his laboratory one of the authors received much inspiration, and his elegant studies on the rearrangement of substituted vinylcyclopropanes stimulated the author's work on these substrates.

REFERENCES

1. (a) Forrester, R. A.; Ishizu, K.; Kothe, G.; Nelsen, S. F.; Ohya-Nishiguchi, H.; Watanabe, K.; Wilker, W. Organic Cation Radicals and Polyradicals. In *Landolt Börnstein, Numerical Data and Functional Relationships in Science and Technology*; Springer Verlag: Heidelberg, 1980; Vol. IX, Part d2. (b) Yoshida, K. *Electrooxidation in Organic Chemistry: The Role of Cation Radicals as Synthetic Intermediates*; Wiley: New York, 1984. (c) Shida, T. *Electronic Absorption Spectra of Radical Ions*; Elsevier: Amsterdam, 1988. (d) *Radical Ionic Systems*; Lund, A.; Shiotani, M., Eds., Kluwer Academics: Dordrecht, 1991.
2. (a) Ledwith, A. *Acc. Chem. Res.* **1972**, *5*, 133. (b) Shida, T.; Haselbach, E.; Bally, T. *Acc. Chem. Res.* **1984**, *17*, 180-186. (c) Nelsen, S. F. *Acc. Chem. Res.* **1987**, *20*, 269-276. (d) Roth, H. D. *Acc. Chem. Res.* **1987**, *20*, 343-350. (e) Bauld, N.; Bellville, D. J.; Harirchian, B.; Lorenz, K.T.; Pabon, R. A.; Reynolds, D.W.; Wirth, D. D.; Chiou, H-S.; Marsh, B. K. *Acc. Chem. Res.* **1987**, *20*, 371. (f) Gerson, F. *Acc. Chem. Res.* **1994**, *27*, 63. (g) Roth, H. D. *Topics Curr. Chem.* **1992**, *163*, 133-245.
3. quadricyclane to norbornadiene radical cation: (a) Roth, H. D.; Schilling, M. L. M.; Jones, G., II *J. Am. Chem. Soc.* **1981**, *103*, 1246-1248. (b) Roth, H. D.; Schilling, M. L. M. *J. Am. Chem. Soc.* **1981**, *103*, 7210-7217.
methylenecyclopropane rearrangement: (c) Takahashi, Y.; Mukai, T.; Miyashi T. *J. Am. Chem. Soc.* **1983**, *105*, 6511-6513. (d) Miyashi, T.; Takahashi, Y.; Mukai, T.; Roth, H. D.; Schilling, M. L. M. *J. Am. Chem. Soc.* **1985**, *107*, 1079-1080.
bicyclobutane to cyclobutene rearrangement: (e) Gassman, P. G.; Hay, B. A. *J. Am. Chem. Soc.* **1985**, *107*, 4075. (f) Gassman, P. G.; Hay, B. A. *J. Am. Chem. Soc.* **1986**, *108*, 4227. (g) Arnold, A.; Burger, U.; Gerson, F.; Kloster-Jensen, E.; Schmidlin, S. P. *J. Am. Chem. Soc.* **1993**, *115*, 4271-4281.
vinylcyclopropane rearrangement: (h) Dinnocenzo, J. P.; Schmittel, M. *J. Am. Chem. Soc.* **1987**, *109*, 1561-1562. (i) Dinnocenzo, J.P.; Conlon, D. A. *J. Am. Chem. Soc.* **1988**, *110*, 2324-2326.
4. cyclopropane systems: (a) Rao, V. R.; Hixson, S. S. *J. Am. Chem. Soc.* **1979**, *101*, 6458. (b) Hixson, S. S.; Xing, Y. *Tetrahedron Lett.* **1991**, *32*, 173-174. (c) Dinnocenzo, J. P.; Todd, W. P.; Simpson, T. R.; Gould, I. R. *J. Am. Chem. Soc.* **1990**, *112*, 2462-2464. (d) Dinnocenzo, J. P.; Lieberman, D. R.; Simpson, T. R. *J. Am. Chem. Soc.* **1993**, *115*, 366-367.
bicyclobutane systems: (e) Gassman, P. G.; Olson, K. D.; Walter, L.; Yamaguchi, R. *J. Am. Chem. Soc.* **1981**, *103*, 4977. (f) Gassman, P. G.; Olson, K. D. *J. Am. Chem. Soc.* **1982**, *104*, 3740.
vinylcyclobutane systems: (g) Arnold, D. R.; Du, X. J. *J. Am. Chem. Soc.* **1989**, *111*, 7666. (h) Arnold, D. R.; Du, X. *Can. J. Chem.* **1994**, *72*, 403. (i) Zhou, D., Sheikh, M.; Roth, H. D. *Tet. Lett.* **1996**, *37*, 2385.

5. Dass, C.; Peake, D. A.; Gross, M. L. *Org. Mass. Spectrom.* **1986**, *21*, 741-746.
6. Weng, H.; Sheik, Q.; Roth, H. D. *J. Am. Chem. Soc.* **1995**, *117*, 10655-10661.
7. Scott, L. T.; Erden, I.; Brunsvold, W. R.; Schultz, T. H.; Houk, K. N.; Paddon-Row, M. N. *J. Am. Chem. Soc.* **1982**, *104*, 3659.
8. (a) Shchapin, I. Yu.; Fel'dman, V. I.; Belevskii, V. N.; Donskaya, N. A.; Chuvylkin, N. D. *Russ. Chem. Bull.* **1994**, *43*, 1-12. (b) Shchapin, I. Yu.; Fel'dman, V. I.; Belevskii, V. N.; Donskaya, N. A.; Chuvylkin, N. D. *Russ. Chem. Bull.* **1995**, *44*, 203-227.
9. Roth, H. D.; Herbertz, T. unpublished results.
10. Roth, H. D.; Herbertz, T. *J. Am. Chem. Soc.*, **1993**, *115*, 9804-9805.
11. A detailed description of the theoretical methods used in this work is contained in Hehre, W. J.; Radom, L.; Pople, J. A.; Schleyer, P. v. R. *Ab Initio Molecular Orbital Theory*; Wiley Interscience, New York, **1986**.
12. Frisch, M. J.; Trucks, G. W.; Schlegel, H. B.; Gill, P. M. W.; Johnson, B. G.; Robb, M. A.; Cheeseman, J. R.; Keith, T.; Peterson, G. A. Montgomery, J. A.; Raghavachari, K.; Al-Laham, M. A.; Zakrzewski, V. G.; Ortiz, J. V.; Foresman, J. B.; Peng, C. Y.; Ayala, P. Y.; Chen, W.; Wong, M. W.; Andres, J. L.; Replogle, E. S.; Gomperts, R.; Martin, R. L.; Fox, D. J.; Binkley, J. S.; DeFrees, D. J.; Baker, J. P.; Stewart, J. P.; Head-Gordon, M.; Gonzalez, C.; Pople, J. A. *GAUSSIAN 94*; Gaussian, Inc., Pittsburgh, PA.
13. (a) Eriksson, L. A.; Malkin, V. G.; Malkina, O. L.; Salahub, D. R. *J. Chem. Phys.* **1993**, *99*, 9756-9763. (b) Eriksson, L. A.; Malkin, V. G.; Malkina, O. L.; Salahub, D. R. *Int. J. Quantum Chem.* **1994**, *52*, 879-901. (c) Batra, R.; Giese, B.; Spichty, M.; Gescheidt, G.; Houk, K. N.*J. Phys. Chem.* **1996**, *100*, 18371-18379.
14. (a) Haselbach, E. *Chem. Phys. Lett.* **1970**, *7*, 428; (b) Collins, J.R.; Gallup, G. A. *J. Am. Chem. Soc.* **1982**, *104*, 1530; (c) Bouma, W. J.; Poppinger, D.; Radom, L. *Isr. J. Chem.* **1983**, *23*, 21; (d) Wayner, D. D. M.; Boyd, R. J.; Arnold, D. R. *Can. J. Chem.* **1985**, *63*, 3283; *Can. J. Chem.* **1983**, *61*, 2310; (e) Du, P.; Hrovat, D. A.; Borden, W. T. *J. Am. Chem. Soc.* **1988**, *110*, 3405; (f) Krogh-Jespersen, K.; Roth, H. D. *J. Am. Chem. Soc.* **1992**, *114*, 8388-8394.
15. (a) Roth, H. D.; Schilling, M. L. M. *J. Am. Chem. Soc.* **1980**, *102*, 7956-7958. (b) Roth, H. D.; Schilling, M. L. M. *J. Am. Chem. Soc.* **1983**, *105*, 6805. (c) Roth, H. D.; Schilling, M. L. M. *Can. J. Chem.* **1983**, *61*, 1027.
16 (a) Iwasaki, M.; Toriyama, K.; Nunome, K. *J. Chem. Soc., Chem. Commun.* **1983**, 202. (b) Qin, X. Z.; Snow, L. D.; Williams, F. *J. Am. Chem. Soc.* **1984**, *106*, 7640-7641.
17. Closs, G. L. *Adv. Magn. Reson.* **1974**, *7*, 157-229.
18. Kaptein, R. *Adv. Free Radical Chem.* **1975**, *5*, 319-480.
19. Adrian, F. J. *Rev. Chem. Intermed.* **1979**, *3*, 3-43.
20. Freed, J. H.; Pederson, J. B. *Adv. Magn. Reson.* **1976**, *8*, 2-84.
21. (a) Doering, W. von E.; Lambert, J. B. *Tetrahedron* **1963**, *19*, 1989-1994. (b) Doering, W. von E.; Schmidt, E. K. G. *Tetrahedron* **1971**, *27*, 2005-2030.
22. (a) Blois, M. S., Jr.; Brown, H. W.; Maling, J. E. Proceedings, Neuviéme Colloque Ampére, Geneva, Librairie Payot, 1960, p. 243. (b) Assumed in analogy to typical hydrocarbon radical ions.[19a]

23. Mitzner, B. M.; Theimer, E. T. *J. Org. Chem.* **1962**, *27*, 3359.
24. Miyashi, T.; Takahashi, Y.; Mukai, T.; Schilling, M. L. M.; Roth, H. D. *J. Am. Chem. Soc.* **1985**, *107*, 1079-1080.
25. Rentzepis, P. M.; Steyert, D. W.; Roth, H. D.; Abelt, C. J. *J. Phys. Chem.* **1985**, *89*, 3955-3960.
26. Goez, M.; Frisch, I. *J. Am. Chem. Soc.*, **1995**, *117*, 10486-10502.
27. Arnac, M.; Verboom, G. *Anal. Chem.* **1977**, *49*, 806.
28. Sullivan, A. B.; Reynolds, G. F. *J. Phys. Chem.* **1976**, *80*, 2671.
29. Krynkov, A. I.; Platonova, E. P.; Krasnova, V. A. *Zh. Obshch. Khim.* **1978**, *48*, 2583.
30. Handoo, K. L.; Gadru, K. *Curr. Sci.* **1986**, *55*, 920.
31. Stallings, M. D.; Morrison, M. M.; Sawyer, D. T. *Inorg. Chem.* **1981**, *20*, 2655.
32. (a) Arnold, D. R.; Wong, P. C.; Maroulis, A. J.; Cameron, T. S. *Pure Appl. Chem.* **1980**, *52*, 2609. (b) Klett, M.; Johnson, R. P. *J. Am. Chem. Soc.* **1985**, *107*, 6615.
33. Closs, G. L.; Czeropski, M. S. *Chem. Phys. Lett.* **1977**, *45*, 115-116.
34. Closs, G. L.; Czeropski, M. S. *Chem. Phys. Lett.* **1978**, *53*, 321-324.
35. Kaptein, R. *Nature (London)* **1978**, *274*, 293.
36. Carrington, A.; McLachlan, A. D. *Introduction to Magnetic Resonance*; Harper & Row: N. Y., 1967.
37. Roth, H. D.; Hutton, R. S.; Kraeutler, B.; Cherry, W. R.; Turro, N. J. *J. Am. Chem. Soc.* **1979**, *101*, 2227-2228.
38. Roth, H. D.; Schilling, M. L. M. *J. Am. Chem. Soc.* **1980**, *102*, 4303-4310.
39. Haddon, R. C.; Roth, H. D. *Croat. Chem. Acta* **1984**, *57*, 1165.
40. Dewar, M. J. S.; Dougherty, R. C. *The PMO Theory of Organic Chemistry*, Plenum Press, New York, **1975**.
41. Basch, H.; Robin, M. B.; Kuebler, N. A., Baker, C., Turner, D. W. *J. Chem. Phys.* **1969**, *51*, 52.
42. Lias, S. G.; Bartmess, J. E.; Liebman, J. F.; Holmoes, J. L.; Levin, R. D.; Mallard, W. G. *J. Phys. Chem. Ref. Data 17*: P 861. (**1988**)
43. Heilbronner, E.; Gleiter, R.; Hopf, H.; Hornung, V.; De Meijere, A. *Helv. Chim. Acta* **1971**, *54*, 783.
44. Boche, G.; Walborsky, H. M. *Cyclopropane Derived Reactive Intermediates*; Wiley: Chichester, **1990**; Chapter 5.
45. Coulson, C.; Moffitt, W. *J. Chem. Phys.* **1947**, *15*, 151.
46. Raghavachari, K.; Haddon, R. C.; Roth, H. D. *J. Am. Chem. Soc.* **1983**, *105*, 3110.
47. Roth, H. D.; Schilling, M. L. M.; Raghavachari, K. *J. Am. Chem. Soc.* **1984**, *106*, 253.
48. Raghavachari, K.; Roth, H. D. *J. Am. Chem. Soc.*, **1989**, *111*, 253.
49. (a) Glass, D. S.; Zirner, J.; Winstein, S. *Proc. Chem. Soc.* **1963**, 276. (b) Ellis, R. J.; Frey, H. M. *Proc. Chem. Soc.* **1964**, 221. (c) Roth, W. R. *Liebigs Ann. Chem.* **1964**, *671*, 10. (d) Roth, W. R.; König, J. *Liebigs Ann. Chem.* **1965**, *688*, 28.

(*Received* 4 *December* 1996)